Title
ENGINEERING ANALYSIS OF THE ROTORFERMENTOR

Authors
Margarities, Argyrios
Wilke, Charles R.

Publication Date
1971-08-01

Presented at the Annual Meeting of the
Society for Industrial Microbiology,
Colorado State University, Fort Collins, CO.
August 29-September 4, 1971

ENGINEERING ANALYSIS OF THE ROTORFERMENTOR

Argyrios Margaritis and Charles R. Wilke

August 1971

AEC Contract No. W-7405-eng-48

DISCLAIMER

ENGINEERING ANALYSIS OF THE ROTORFERMENTOR*

Argyrios Margaritis and Charles R. Wilke

Department of Chemical Engineering and Lawrence Berkeley Laboratory
University of California
Berkeley, California 94720

August 1971

ABSTRACT

The Rotorfermentor is a relatively new type of fermentation apparatus in which cells are grown in the annular space surrounding a hollow rotating cylinder (the rotor) covered with a microporous membrane. The cells can be retained in the apparatus by centrifugal and/or filtration action while the metabolic products in the broth are continuously removed through the membrane. This dual function of continuous cell growth and concentration is the essential characteristic of the Rotorfermentor. As a result, high cell concentrations are achieved. Previous research in this laboratory has demonstrated the basic technique.

In this paper an engineering analysis is presented which reviews the basic theoretical principles of the Rotorfermentor design and its operating characteristics. Theoretical equations are presented which give filtration rates for a model Newtonian system of spherical particles under the influence of centrifugal and fluid drag forces and the power consumption of the rotating rotor.

---

* Paper presented at the Annual Meeting of the Society for Industrial Microbiology, August 29-September 4, 1971, Colorado State University, Fort Collins, Colorado.

An equation is presented which relates the cell productivity per unit fermentor volume of the Rotorfermentor with that of an ordinary fermentor. Performance of the Rotorfermentor is also compared with that for a membrane dialysis fermentor system.

The prototype Rotorfermentor consists of a 2-inch diameter rotor of 12 inches height enclosed in the fermentor vessel which has a diameter of 10 inches and height of 12 inches (approximately 12 liters net fermentor volume). A preliminary process engineering analysis suggests that a Rotorfermentor might replace economically both the ordinary fermentor and the centrifuge cell separator in a pilot scale continuous process for endoenzyme production.

Future applications of the Rotorfermentor include the continuous concentration of cell mass and separation of other metabolic products for anaerobic and aerobic systems.

INTRODUCTION

Bacterial concentrations in liquid cultures reach a certain maximum level which is characteristic of the strain and culture conditions. This maximum concentration of microorganisms grown in ordinary batch or continuous culture conditions is usually in the order of a few grams of dry weight of cell mass per liter of broth. Since the rate of bacterial growth in logarithmic phase is proportional to the number of cells present, i.e. autocatalytic growth, then high cell densities could result in great increases of cell productivity per unit fermentor volume.

A review of the literature (4,6,15,17,22) reveals that one or a combination of the following three main factors limit maximum cell concentration: exhaustion of a limiting substrate, accumulation of toxic metabolic end product(s), and lack of available oxygen in the case of aerobic systems. In order to overcome these limiting factors it is necessary to devise special fermentor systems. These systems should provide for continuous feeding of fresh medium, removal of toxic end products from the broth, and adequate oxygen supply.

The Rotorfermentor is a device which is designed to achieve high cell-densities in batch and continuous cultures by removal of toxic metabolic end products continuously through a rotating filtration membrane. Use of this device was first suggested by Bhagat and Wilke (2) and subsequently employed by Sortland and Wilke (24) to produce high density cultures of Streptococcus faecalis.

In addition to cell production, the Rotorfermentor can be used for the production of metabolic products excreted by the organism into the broth.

These products can be separated from the cells by filtration through the membrane. The dual function of the Rotorfermentor, i.e. cell growth and high cell concentration might be used to replace both an ordinary C.S.T. fermentor and a cell centrifuge separator in conventional cell production. Another promising application might be the efficient biological transformation of various substrates by the highly-concentrated cell mass.

Further analysis and comparison of various dense cell culture systems is given below.

CONTINUOUS HIGH CELL DENSITY CULTURE SYSTEMS

As shown in Figures 1 and 2, three different fermentor schemes have been proposed to achieve continuous dense cell cultures. Figure 1a shows a scheme where a C.S.T. fermentor is connected with a centrifuge separator with part of the concentrated cells being recycled back into the fermentor. A theoretical treatment of the performance of this scheme is given by Herbert (13). The main difficulty with this system is that a good part of toxic end products are recycled back into the fermentor along with the cells. In addition, the cells are exposed continuously to two different environments, one the fermentor and the other being the centrifuge separator where there is no provision for either substrate addition or any aeration at all. Especially at high cell densities the microorganism may experience nutrient and/or oxygen "shock" during the time it spends in the centrifuge and recycle lines.

Gerhardt et al. (8,21) developed the continuous dialysis fermentor scheme shown in Figure 1b. The basic characteristic of this technique is the use of a dialysis membrane which separates the fermentor from the nutrients reservoir. The membrane is mounted on a plate and frame type dialyzer and continuous circulation of the nutrients and bacterial culture is achieved on either side of the membrane as shown in Figure 1b.

The nutrients diffuse through the dialysis membrane into the fermentor while the metabolic end products counterdiffuse through the membrane from the fermentor to the reservoir. For the continuous mode of operation, the bacteria in the fermentor have two sources of substrate, one from diffusion through the membrane and the other from the direct feed into the fermentor. According to Schultz and Gerhardt (21), it is this extra source of substrate

through the dialysis membrane which gives higher cell densities than those obtained when using an ordinary C.S.T. fermentor. For example, from Figure 3b we see that the computed maximum cell productivity of a hypothetical organism used by Herbert et al. (14) occurs at the dilution rate, D, of approximately 0.85 hr^{-1}. At this dilution rate the cell productivity of the continuous dialysis fermentor system is about 5 g cells/hr and that of an ordinary fermentor (non-dialysis) 3.8 g cells/hr, i.e. a ratio of 1.3. The corresponding computed cell densities at D = 0.85 hr^{-1} are 5.6 g cells/liter for the dialysis system, and 4.3 g cells/liter for the ordinary fermentor. Much higher cell densities are achieved at lower dilution rates but this is done at the expense of lower substrate utilization efficiencies (% substrate converted to cell mass). For example, at D = 0.2 hr^{-1} from Figure 3a, $X \simeq 11$ g cells/liter for the dialysis fermentor and $X \simeq 5$ g cells/liter for the ordinary (non-dialysis) C.S.T. fermentor, i.e. a ratio of approximately 2.2. The corresponding substrate utilization efficiencies, Figure 3c at D = 0.2 hr^{-1} are approximately 100% for the ordinary (non-dialysis) fermentor, and about 60% for the dialysis continuous fermentor. If substrate costs are high, the gain in cell productivity of the dialysis system might be offset by substrate losses.

A limitation of the dialysis fermentor is the inherently slow process of diffusion of both nutrients and metabolic products through the dialysis membrane. If the rate of diffusion of toxic metabolic products out of the apparatus is less than the rate of their production by the cells, then the toxic product concentration in the fermentor may reach high levels, thereby limiting maximum cell concentration. This may explain the fact that Gerhardt and Gallup (10) obtained very low cell concentration of Streptococcus lactis (lactic

acid inhibitor) as compared with high cell densities obtained for Serratia marcescens 8UK in their flask dialysis experiments.

Figure 2 shows a schematic of the Rotorfermentor. It consists of three main parts: the rotating cylindrical rotor, the fermentor vessel, and the filtrate chamber on top which is separated from the fermentor. The rotor is connected to a variable speed motor unit and a microporous filtration membrane is attached to the rotor. There is an annular space between the membrane and the rotor which allows for the flow of filtrate from the fermentor through the membrane and into the filtrate chamber. Any gas trapped in the filtrate separates out and leaves at the top of the filtrate chamber while the liquid filtrate is withdrawn at the bottom as shown. The air and liquid medium are supplied under pressure through a special sparger system at the bottom of the fermentor. This pressure provides the necessary driving force for filtration through the microporous membrane at a given rotational speed of the rotor. A small recycle line is used to remove gas (air) and also withdraw the concentrated cells through the cell bleed line. Any toxic metabolic products produced by the cells are continuously removed through the filtration membrane while the concentrated cells inside the fermentor are replenished with fresh medium. Sortland and Wilke (24) used the same technique but a different design version to study the growth characteristics of a strain of Streptococcus faecalis. This anaerobic homo-fermentative bacterium ferments 90-95% of the glucose to lactic acid via the Embden-Meyerhoff pathway according to Gunsalus and Niven (11). In this case the removal of lactic acid is necessary if high cell densities are desired. Sortland and Wilke (24) used a 0.45 micron Millipore membrane and were able to obtain 40% packed cell volume using the fermentor-rotor scheme under semi-

batch operating conditions, i.e. continuous feed and filtration but no cell bleed. This corresponds to 94 g cells/liter (oven dry basis). Under ordinary batch conditions with the rotor removed from the fermentor, 2.1 g cells/liter were obtained, which represents a ratio in cell concentrations of approximately 45 when compared with the rotorfermentor.

In addition, the rotorfermentor was operated continuously and a steady-state value of approximately 52 g cells/liter was obtained. The steady-state continuous operation without the rotor (ordinary C.S.T. fermentor) gave a maximum cell concentration of about 1.9 g cells/liter. Therefore, under similar continuous operating conditions the rotorfermentor gave cell cultures about 27 times more concentrated than those obtained using an ordinary fermentor. Figure 4 shows the 40% packed cell volume culture obtained by Sortland and Wilke (23).

OPERATIONAL CHARACTERISTICS OF THE ROTORFERMENTOR

The new design of the Rotorfermentor presently under construction is a modification of the original filtration-fermentor employed by Sortland and Wilke (24), which provides larger fermentor capacity. In addition, air supply through a special sparger system extends the application to aerobic systems.

As shown in Figure 2, the system consists of the fermentor vessel which has a diameter of 10 inches and 12 inches height giving approximately 12.85 liters volume. The rotor has a 2-inch diameter and 12-inch height giving approximately 0.62 liter volume and available membrane filtration area is 486 cm^2. The net available fermentor volume is about 12 liters when the rotor volume and oxygen probe plus cooling coil volumes are subtracted from the original 12.85 liters. The filtration chamber has a diameter of 12 inches and approximately 9 inches height. The rotor is supported at both ends by means of two sets of Crane seals and self-lubricating ball bearings, and it is connected at the bottom to a variable-speed motor unit which has a maximum speed of 4,500 revolutions per minute (r.p.m.).

Two positive displacement metering Moyno pumps are used, one for the recycle line and the other for the withdrawal of cell bleed. A pressurized stainless steel tank is used for the nutrients supply and a variable pressure air source is used with a special sparger mounted at the bottom of the fermentor.

Strong turbulent mixing of the liquid broth is achieved by means of the rotating rotor. Additional bulk mixing is created by the recycling of the broth. When the rotor is operated at its maximum speed of about 4,500 r.p.m., the maximum pressure inside the fermentor required to overcome the centrifugal

force during filtration is about 10 p.s.i.g. Temperature control and pH control are also provided. The pressure inside the fermentor is controlled by means of a control valve. The oxygen partial pressure in the liquid broth inside the fermentor is measured by means of a steam-sterilizable Fermentation Design teflon probe.

At a given pressure level inside the fermentor vessel, the Rotor-fermentor can be operated in two ways: (1) filtration with cake formation at the membrane surface or (2) filtration with no cake formation. In the latter case the centrifugal force field created by the rotor prevents particles from reaching the membrane surface. An analysis of both modes of filtration is given below. Figure 5 shows the assembled Rotorfermentor.

In the case of steady-state operation of a C.S.T. fermentor, the dilution rate D is always equal to the specific growth rate μ, and cell washout will occur at $D > \mu_{max}$.

The dilution rate of the Rotorfermentor is $D_r = B/V_r$ which is not identical with the overall dilution rate, D_o, defined by Equation 1,

$$D_o = \frac{\text{total flow through the Rotorfermentor}}{\text{fermentor volume}} = \frac{F_r}{V_r} . \qquad (1)$$

At steady-state operation

$$F_r = B + L . \qquad (2)$$

Assuming no cells in the filtrate and from a cell mass balance with $D_r = \mu$, divide Equation 2 by V_r to get Equation 3,

$$D_o = \mu + \frac{L}{V_r} . \qquad (3)$$

As seen from Equation 3 at steady-state operation of the Rotorfermentor the overall dilution rate is always greater than μ. When $D_o > \mu_{max}$ no cell washout occurs provided $D_r \leq \mu_{max}$. This is due to the fact that the cells are retained in the fermentor by the filtration membrane. However, cell washout will occur when $D_r > \mu_{max}$.

FILTRATION MEMBRANES

Filtration rates through the rotating filter membrane may become the limiting step in attaining very high cell concentrations in the Rotorfermentor. Use of metallic microporous membranes with rigid smooth surfaces offers promising possibilities at high enough rotor speeds to prevent cake build-up at the membrane surface.

A preliminary screening of some of the existing metallic membranes of various pore sizes gave the results shown in Figure 6, where the filtration rate of pure water per unit membrane area is plotted against pressure drop across the membrane. The first membrane is a stainless steel smooth membrane of 0.01 inch thickness made by Mallory Metallurical Co. with a wide range of pore sizes from 100 to 400 microns, with the mean pore size close to about 250 microns, and 10% open area. Two other membranes made of 1/16-inch sintered stainless steel are also shown; one is Grade F of 20 micron pores and the other is Grade H of 5 micron pores. For comparative purposes a Millipore cellulose acetate membrane grade WS of 3-micron pore size is also shown. Plastic membranes of pore sizes less than 1 micron might be supported between two metallic membranes of very large pore sizes and having more than 80% open area. In this way high rotational speeds may be attained without damaging the plastic membranes by fluid friction.

HYDRODYNAMIC CHARACTERISTICS OF THE ROTORFERMENTOR

When the cylindrical membrane rotates the fluid elements adjacent to the membrane surface are also subjected to rotational motion. At low rotor speeds laminar flow conditions exist in the annulus between the rotor surface and the wall of the fermentation chamber. This case is adequately described by Schlicting (20). However, as the rotor speed is increased, a critical value is reached beyond which fully turbulent flow conditions are developed in the annulus. Turbulence in the vicinity of the rotor is characterized by the dimensionless Taylor Number, T, defined by Equation 4,

$$T = \frac{4}{9} D^4 \left(\frac{\omega}{\nu}\right)^2 \tag{4}$$

where

D = rotor diameter, cm

$\omega = 2\pi N$ = angular velocity of rotor, radians/sec

N = revolutions per sec, sec^{-1}

$\nu = \mu/\rho$ = kinematic viscosity, cm^2/sec

μ = viscosity of fluid, g/cm sec

ρ = density of fluid, g/cm^3.

According to Chandrasekhar (3) the critical Taylor Number, T_c, beyond which turbulence occurs is equal to 3.1×10^4, although the critical Taylor Number is also a function of the annulus width. At rotor speeds well beyond the critical value Donelly and Simon (5) obtained an empirical relationship between the angular velocity, ω, annulus width, d, and the torque transmitted by the rotor to the fluid. Batchelor (1) provides a theoretical analysis of

the experimental results, postulating a steady flow pattern in the axial plane passing through the annulus as shown in Figure 7.

The peripheral velocity of the fluid elements adjacent to the membrane varies with distance. At very small distances away from the membrane surface, i.e. about 50 microns or less, the fluid elements do not "see" the membrane curvature. Therefore, in order to simplify the analysis a good approximation can be made by neglecting the membrane curvature and assuming flow past a flat plate. For turbulent flow conditions past a flat plate the velocity profile in the boundary layer is given by Von Karman's (26) universal velocity profile in the form:

$$v = v_o (1 - ax) \tag{5}$$

where

v = peripheral (tangential) velocity of liquid element at distance x from the membrane surface, cm/sec

v_o = peripheral velocity of membrane, cm/sec = πDN

$a = \frac{\tau_w g_c}{\mu v_o}$, cm^{-1}

τ_w = shear stress at the membrane surface, $g/cm^2 = \left(\frac{f}{2}\right)\left(\frac{\rho v_o^2}{g_c}\right)$

f = friction factor, a function of Reynolds No.

g_c = gravitational constant = 980 cm/sec^2 .

In the derivation of Equation 5 it is assumed that there is no appreciable effect of the fluid radial flow on the peripheral velocity profile.

Figure 8 is a plot of the Von Karman velocity profile for two different viscosities at various speeds of the 2-inch diameter rotor.

Another important variable is the power consumed by the rotor which is transmitted to the fluid in the annulus. The power consumption is a function of the rotor geometry and speed, and the physical properties of the fluid. Equation 6 shows the power consumption for a cylinder rotating in a Newtonian fluid, under fully turbulent flow conditions.

$$P = (1.272 \times 10^{-8}) (f\rho LD^4N^3) \quad (6)$$

where

P = power consumption, H.P.

ρ = density of fluid, lb/ft^3

f = friction factor

L = length of cylinder, ft

D = diameter of cylinder, ft

N = rotational speed of cylinder, R.P.M.

Figure 9 is a plot of rotor speed against power consumed for various rotor diameters from 1 to 8 inches calculated for a system of 6 centipose viscosity, corresponding in properties to the 40% packed cell volume suspension of Streptococcus faecalis obtained by Sortland (23). Values of the friction factor at different Reynold's Nos. were obtained from Theodorsen and Regier (25).

In the case of aeration the effect of gas bubbles on performance of the Rotorfermentor is not known. Further study will be required to determine whether the bubbles will interfere with passage of liquid through the membrane or reduce the effectiveness of cell retention in the annular space. Another consideration in aerated systems is the effect of the gas phase on power requirements.

THEORY OF FILTRATION THROUGH THE ROTOR MEMBRANE

Consider any particle in the boundary layer near the membrane surface moving with a peripheral velocity v at a distance r from the rotor axis. The particle is subjected to a centrifugal force F_c given by Equation 7.

$$F_c = (m_{eff})\left(\frac{v^2}{r\, g_c}\right) \tag{7}$$

where

m_{eff} = effective particle mass, $g = \frac{\pi}{6} D_p^3 (\rho_p - \rho)$, for spheres

F_c = centrifugal force, g_f

D_p = particle diameter, cm

ρ_p = particle density, g/cm^3

ρ = density of the fluid, g/cm^3 .

Substituting for v from Equation 5 and rearranging, we get

$$F_c = \left(\frac{\pi}{6} D_p^3 \Delta\rho\right)\left(\frac{v_o^2}{r\, g_c}\right)(1 - ax)^2 \tag{8}$$

where

$$\Delta\rho = \rho_p - \rho \ .$$

The centrifugal force tends to throw the particle away from the membrane surface. If at the same time there is a filtrate flow radially into the membrane, the particle experiences a drag force, F_D, which tends to carry the particle towards the membrane. The drag force acting on the particle is given by Equation 9.

$$F_D = \left(\frac{C_D}{2g_c}\right)(A_p \rho\, \dot{u}^2) \tag{9}$$

where

C_D = drag coefficient, a function of the particle Reynold's No. Re_p and

$$Re_p = \frac{D_p u}{\nu}$$

A_p = projected area of particle in the direction of motion, cm^2

$$A_p = \frac{\pi D_p^2}{4} \quad \text{for spherical particles}$$

u = radial liquid velocity, cm/sec; also u = $cm^3/sec\ cm^2$, i.e. filtrate flux through the membrane.

For small relatively light particles, as in the case of bacteria, the gravity and buoyancy forces acting are negligible compared with the two dominant forces F_c and F_D. Furthermore, for small values of u, so that $Re_p < 0.03$, we assume viscous flow and Stoke's Law is applicable.

$$C_D = \frac{24}{Re_p} = \frac{24\mu}{\rho D_p u} \tag{10}$$

Substituting Equation 10 into Equation 9 gives

$$F_D = \left(\frac{3\pi}{g_c}\right)(\mu D_p u) \quad . \tag{11}$$

From Equations 8 and 11 we see that for a given set of filtration conditions, the particle size D_p is important since F_c is proportional to D_p^3, while F_D is proportional to D_p. For a given particle size and density, F_c can be changed by varying the rotor speed, N, while F_D can be controlled independently through u by changing the pressure inside the fermentation vessel.

Dividing Equation 7 by Equation 11 and noting that $r = R_o + x \simeq R_o$, since the rotor radius $R_o >> x$, we get Equation 12,

$$\frac{F_c}{F_D} = \left(\frac{\Delta\rho}{18\mu u R_o}\right)(D_p^2 v^2) \quad . \tag{12}$$

If $F_c > F_D$ at the membrane surface, i.e. $x = 0$, particles in the liquid will not reach the surface, but rather will reach an equilibrium position at a distance $x = x_{equ}$, where $F_c = F_D$. It is assumed that the particles are carried by the fluid at the same peripheral velocity which varies with distance according to Equation 5. This mode of operation prevents the particles from touching the membrane surface and thus prevents cake formation or possible plugging of membrane pores. The higher the F_c/F_D ratio at $x = 0$, the greater the equilibrium distance x_{equ}, and theoretically a clear boundary layer region free of particles could exist adjacent to the membrane surface. In this case it would be possible to use membranes with large pores with corresponding large filtration rates. We shall call this mode of operation "centrifugal" filtration. Equation 12 does not include particle to particle interaction and is applicable only to Newtonian fluids. For a given set of values of $\Delta\rho$, μ, R_o, and equilibrium conditions such that $F_c/F_D = 1$, Equation 12 can be used to predict theoretical filtration rates, u, at different values of D_p and v. Such a plot of v versus u at different D_p values for the 2-inch rotor is shown in Figure 10.

A preliminary test run was made using Bhagat's (2) modified apparatus equipped with a 6-inch diameter rotor and the 10% open area Mallory metallic membrane of average pore size of about 250 microns. The flow diagram was the same as that shown in Figure 2 without the recycle. Polystyrene spheres of size

range 6 to 14 microns were used. The rotor speed was 2,500 R.P.M. and the filtration rate $u = 4.69 \times 10^{-2}$ $cm^3/sec\ cm^2$ or 0.691 $gal/min\ ft^2$. The experimental results are shown in Figure 11. In this case the bleed rate was zero and the concentration inside the vessel increased linearly with time in agreement with a mass balance for the particles. Calculations showed that particles of size 10 microns or less were not subjected to sufficiently high centrifugal forces to prevent them from going through the large membrane pores. A travelling probe was used to take samples at various distances x from the membrane surface. As shown from Figure 11 there was no concentration gradient, an indication of good mixing conditions in the annulus.

If $F_c < F_D$ at the membrane surface, i.e. $x = 0$, the particles will touch the surface with resultant cake formation, provided the pore size of the membrane is smaller than the particle size so that the particles do not go through. For a given R.P.M. and pressure inside the vessel at the beginning of a steady-state run, the cake thickness will start building up until a constant thickness is achieved. Correspondingly the filtration rate will be high at the beginning and then decrease slowly until it reaches a limiting constant value, u_∞. This type of filtration we shall call "cake" filtration. Bhagat and Wilke (2) developed a model which includes the effects of centrifugal and drag forces as well as the diffusion of particles away from the cake to the bulk of the fluid. This theoretical model is shown in Figure 12. The convective flux is due to bulk fluid flow through the cake and membrane, the diffusion flux includes both eddy and molecular diffusion and is due to the concentration gradient of particles, and the centrifugal flux is due to centrifugal force. At steady-state conditions, the convective flux must equal the

diffusion flux plus the centrifugal flux. Using this type of analysis, Bhagat and Wilke (2) were able to explain why the steady-state limiting filtration rates obtained in their experiments were greater than those predicted by Equation 12. Figure 13 shows typical experimental results obtained by Bhagat and Wilke (2) using a 6-inch rotor and a Millipore membrane grade WH of 0.45 micron pore size. The particles used were Dow polystyrene of 1.3 micron size and 1.056 g/cm^3 density. For this run the rotor speed was maintained constant at N = 1,200 R.P.M. and the filtrate flow rate at two filtration pressures 10.4 p.s.i.g. and 13.4 p.s.i.g. was measured as a function of time. As seen from Figure 13, the filtrate flow rate starts at a high value, then as the cake builds up, the flow rate decreases to reach a terminal constant value. Increasing the pressure to a higher value, i.e. 13.4 p.s.i.g. momentarily increases the flow rate but it levels off to the original value as the new higher cake thickness offsets the new higher filtration pressure, while maintaining the rotor speed constant. Bhagat and Wilke (2), in general, found that

$$u_\infty \propto \left(\frac{\Delta P\ N^2}{\ell}\right) \tag{13}$$

where

u_∞ = limiting filtrate flux, $cm^3/sec\ cm^2$

ΔP = pressure drop across cake and membrane, p.s.i.g.

N = rotor speed, R.P.M.

ℓ = cake thickness, cm .

COMPARISON OF THE ROTORFERMENTOR WITH THE C.S.T. FERMENTOR

One of the major advantages of the Rotorfermentor is high cell productivities per unit fermentor volume. An expression can be developed which relates the cell productivity of the Rotorfermentor to that of an ordinary C.S.T. fermentor. The two schemes are shown in Figure 14.

The cell productivity of the C.S.T. fermentor is given by Equation 14,

$$Q = \frac{FX}{V} \tag{14}$$

where

Q = cell productivity, g cells/lit hr

F = volumetric feed flow rate, lit/hr

V = volume of the C.S.T. fermentor, lit

X = cell concentration, g cells/lit .

The cell productivity for the Rotorfermentor is given by Equation 15,

$$Q_r = \frac{BX_r}{V_r} \tag{15}$$

where

Q_r = cell productivity of the Rotorfermentor, g cells/lit hr

B = volumetric cell bleed rate, lit/hr

V_r = net fermentor volume of the Rotorfermentor, lit

X_r = cell concentration, g cells/lit .

The cell productivity ratio of the Rotorfermentor to C.S.T. fermentor, R, is given by

$$R = \left(\frac{B\ V}{V_r F}\right)\left(\frac{X_r}{X}\right) . \tag{16}$$

At steady-state the specific growth rate for each system is given by

$$\mu = \frac{F}{V} = \frac{B}{V_r} . \tag{17}$$

If it is assumed that the Rotorfermentor is operated at the same specific growth rate as the C.S.T. fermentor, Equation 16 becomes

$$R = \frac{X_r}{X} . \tag{18}$$

For the C.S.T. fermentor the cell concentration is given by

$$X = Y_{x/s}\ (S_o - S_1) \tag{19}$$

where

S_o = concentration of limiting substrate in the feed

S_1 = concentration of limiting substrate in the fermentor

$Y_{x/s}$ = cell mass to substrate yield coefficient .

Similarly for the Rotorfermentor a material balance at steady-state gives

$$X_r = Y_{x/s}\ (S_o - S_1) \cdot \frac{F_r}{B} . \tag{20}$$

Therefore, if the two fermentors are operated at the same level of substrate concentration, i.e. a condition imposed by Equation 17 and assuming the same yield coefficients, Equations 19 and 20 may be combined to give

$$\frac{X_r}{X} = \frac{F_r}{B} = 1 + \frac{L}{B} . \tag{21}$$

As shown by Equations 20 and 21 high cell concentrations and high productivity ratios are attained in the Rotorfermentor by employing a high ratio of feed rate to bleed rate. Thus by suitable choice of flow rates, the Rotorfermentor may fulfill the functions of both an ordinary fermentor and centrifuge cell separator.

In a conventional process where an endocellular product is desired, the first step is cell production in a fermentor followed by cell concentration in a centrifuge, cell disruption and further separation and purification of the final product. Such a process for the continuous pilot scale production of an endoenzyme is described by Lilly and Dunnill (16) employing a wild-type Pseudomonas aeruginosa, a facultative aerobe, to produce the endocellular enzyme amidase. Figure 15a shows part of the flowsheet based on the given information (16). A C.S.T. 100-liter fermentor was used at a dilution rate $D = 0.4\ hr^{-1}$ for maximum enzyme output. The cell concentration leaving the fermentor was 2-3 g cells/lit (oven dry basis). The cells were then fed to a Westphalia centrifuge separator model SAOOH-205, which produced a cell slurry of 15 to 25 g cells/lit, i.e. a concentration factor of 6 to 8 times. According to information supplied by the manufacturer (private communication) the Westphalia centrifuge separator model SAOOH-205 separates about 80% to 90% of the cells entering. Based on this information, a cell mass balance was made around the centrifuge as shown in Figure 15a. The concentrated cell output coming out of the centrifuge is estimated to be 96 g cells/hr.

Figure 15b shows the operating conditions of a 12-liter Rotorfermentor (10 liter working volume) designed to give the same cell output as that obtained in Figure 15a, i.e. 96 g cells/hr at the same specific growth rate, $0.4\ hr^{-1}$,

and the same substrate concentration in the feed. Assuming practically all substrate is converted to cell mass, the cell concentration inside the Rotorfermentor, X_r, is 24 g cells/lit, and the feed and filtrate rates, F_r and L, are 32 lit/hr and 28 lit/hr, respectively. The specified cell concentration is well below the experimental value of 52 g cells/lit obtained by Sortland and Wilke (23) for continuous Rotorfermentor operation with Streptococcus faecalis.

According to information obtained from the manufacturer (private communication), the Westphalia centrifuge model SA00H-205 draws 1.5 H.P. power at the start and about 0.9 H.P. once it reaches its final rotational speed. At a typical power input of 3 H.P. per 1,000 gallons liquid for the C.S.T. fermentor and 60% mechanical efficiency, the 100-liter fermentor consumes about 0.13 H.P. Therefore, for the Westphalia and C.S.T. fermentor the total power consumed is 1.03 H.P. to produce 96 g cells/hr. The energy consumed to produce and concentrate the cells is therefore 3.7 Kwatt-hr/lb cell mass.

In the case of the Rotorfermentor the rotor has a diameter of 3 inches and 24 inches height giving a filtration area of 1,460 cm^2. To maintain a filtrate rate of 28 lit/hr without cake formation (see Figure 10) for 1 micron particles at μ = 6 c.p., a peripheral velocity of 2,000 cm per second is required, corresponding to N ≃ 5,000 R.P.M. From Figure 9 the power consumed by the rotor, P, is 7.95 H.P., which corresponds to 7.43×10^5 ft-lb_f/min ft^3 liquid in the Rotorfermentor. Therefore, the energy consumed to produce and concentrate the cells in the Rotorfermentor is 28.7 Kwatt-hr/lb cell mass. Thus, for the present example, the Rotorfermentor consumes about 7.7 times more power to do the same job as the C.S.T. fermentor and centrifuge.

The power consumed by the Rotorfermentor is reduced appreciably as the cell size increases. For example, in the above system, if the microorganism size were increased to 5 microns, and for process conditions identical to those given in Figure 15, the same filtration rate could be obtained, i.e. 28 lit/hr in the Rotorfermentor at 1,130 R.P.M. instead of 5,000. This reduction in rotor speed would reduce the power consumption from 7.95 H.P. to about 0.133 H.P. corresponding to 0.48 Kwatt-hr/lb cell mass.

An additional condition pertaining to power input is that sufficient agitation must be provided to disperse oxygen and other substrate constituents throughout the cell suspension at a rate sufficient to sustain the required growth rate. In aerobic systems oxygen supply is usually the limiting factor.

The rate at which oxygen must be supplied to a cell suspension is determined by the respiration rate of the microorganism and the cell concentration. At steady-state this rate must equal the rate of oxygen transfer from the air bubbles to the gas-liquid interface in the fermentor. This relationship is given by Equation 22

$$(k_L a)(C^* - C_B) = Q_m X \qquad (22)$$

where

$k_L a$ = mass transfer coefficient, hr^{-1}

C^* = equilibrium concentration of oxygen, m mole O_2/lit

C_B = oxygen concentration in the bulk of liquid, m mole O_2/lit

Q_m = specific oxygen demand of microorganism, m mole O_2/g cell hr

X = cell concentration, g cell/lit .

Hegeman (private communication, University of California, Berkeley) reports that in the case of Pseudomonas aeruginosa approximately 40% of the substrate carbon in the form of succinate is assimilated to form cell mass and the remainder is oxidized. Therefore, for the C.S.T. fermentation conditions reported by Lilly and Dunnill (16), a value of Q_m may be estimated to be 7.5 m moles O_2/g cells hr. From Equation 22 the required value of k_La is 695 hr^{-1} in order to sustain a cell concentration X_r = 24 g cells/lit in the Rotorfermentor. This value of k_La seems readily attainable at the power input specified above on the basis of existing mass transfer correlations for agitated fermentor vessels (18,19).

CONCLUSIONS

From the foregoing analysis, it may be concluded that the Rotorfermentor is capable of simultaneous growth and concentration of microorganisms. While the power consumption for small size microorganisms is high, this may be offset in particular applications by the small fermentor volume and resulting high cell concentrations obtained. For the pilot scale process comparison of amidase production described above capital equipment costs for the Rotorfermentor system are estimated to be approximately one third of that for a C.S.T. unit plus centrifuge. Further work is needed to determine more accurate power requirements, filtration rates and overall capital costs for large scale processes.

In addition to potential processing applications, the Rotorfermentor is of interest as a research tool for the study of cell growth kinetics and product formation (24). The device is of particular interest for study of the properties of dense cell cultures and the production of metabolic products excreted by the cells when employment of dense cultures would be advantageous. Specific applications of the Rotorfermentor might include the following:

1) Continuous production and concentration of cell mass. Examples: vaccines, other cells.
2) Production and removal through the membrane of cell-free metabolic products excreted by the cell into the liquid broth. Examples: exoenzymes, antibiotics such as penicillin, etc.
3) Biological transformation of various substrates by the highly concentrated cell mass. Examples: steroid hydroxylation, antibiotics transformation, etc.

4) Production of metabolic products present within the cell. Examples: endoenzymes, proteins, nucleic acids, vitamins, etc.

ACKNOWLEDGMENTS

This work was performed under the auspices of the U. S. Atomic Energy Commission.

REFERENCES

1. Batchelor, G. K., "A Theoretical Model of the Flow at Speeds Far Above the Critical", J. Fluid Mechanics 7: 416-418 (1960).

2. Bhagat, A. K. and Wilke, C. R., "Filtration Studies with Ultrafine Particles", Lawrence Radiation Laboratory Report UCRL-16574 (1966).

3. Chandrasekhar, S., "The Stability of Viscous Flow Between Rotating Cylinders", Proceedings of the Royal Society, London, A246: 301-311 (1958).

4. Dagley, S., Dawes, A., and Foster, S. M., "The Influence of pH Value and Aeration on the Growth of Aerobacter Aerogenes and Bacterium Coli in Defined Media", J. Gen. Microbiol. 8: 314-322 (1953).

5. Donnely, R. J. and Simon, N. J., "An Empirical Torque Relation for Supercritical Flow Between Rotating Cylinders", J. Fluid Mechanics 7: 401-416 (1960).

6. Finn, R. K., "Inhibitory Cell Products: Their Formation and Some New Methods of Removal", J. Ferm. Technol. 44: 305-310 (1966)

7. Freter, R. and Ozawa, A., "Explanation for Limitation of Populations of E. Coli in Broth Cultures", J. Bacteriol. 86: 904-910 (1963).

8. Gallup, D. M. and Gerhardt, P., "Dialysis Fermentor Systems for Concentrated Culture of Microorganisms", Appl. Microbiol. 11: 506-512 (1963).

9. Gerhardt, P. and Schultz, J. S., "Dialysis Culture", J. Ferment. Technol. 44: 349-356 (1966).

10. Gerhardt, P. and Gallup, D. M., "Dialysis Flask for Concentrated Culture of Microorganisms", J. Bacteriol. 86; 919-929 (1963).

11. Gunsalus, I. C. and Niven, C. F., "The Effects of pH on the Lactic Acid Fermentation", J. Biol. Chem. 145: 131 (1942).

12. Harrison, D. E. F., and Pirt, S. J., J. Gen. Microbiol. 46: 193-211 (1967).

13. Hebert, D., "A Theoretical Analysis of Continuous Culture Systems", Society of Chemical Industry Monograph, No. 12, pp. 21-53, Page Bros. Ltd, London (1961).

14. Herbert, D., Elsworth, R., and Telling, R. C., "The Continuous Culture of Bacteria; a Theoretical and Experimental Study", J. Gen. Microbiol. 14: 601-622.

15. Hinshelwood, C. N., "The Chemical Kinetics of the Bacterial Cell", The Clarendon Pres, Oxford, England (1946).

16. Lilly, M. D. and Dunnill, P., "Isolation of Intracellular Enzymes From Microorganisms--The Development of a Continuous Process", Fermentation Advances, D. Perlman, editor, Academic Press, New York (1969), pp. 225-247.

17. Monod, J., "The Growth of Bacterial Cultures", Ann. Rev. Microbiol. 3: 371-394 (1949).

18. Robinson, C. W. and Wilke, C. R., "Mass Transfer Coefficients and Interfacial Area for Gas Absorption by Agitated Aqueous Electrolyte Solutions", Lawrence Radiation Laboratory Report UCRL-20472 (April 1971).

19. Robinson, C. W. and Wilke, C. R., "Mass Transfer Coefficients and Interfacial Area for Gas Absorption by Agitated Aqueous Electrolyte Solutions", Chemical Engineering Conference, Sydney and Melbourne, Australia, August 18-26, 1970.

20. Schlicting, H., Boundary Layer Theory, McGraw-Hill Book Co., Inc., New York (1960).

21. Schultz, J. S. and Gerhardt, P., "Dialysis Culture of Microorganisms: Design, Theory, and Results", Bacteriol. Reviews 33: No. 1, 1-47 (March 1969).

22. Sinclair, N. A. and Stokes, J. L., "Factors Which Control Maximal Growth of Bacteria", J. Bacteriol. 83: 1147-1154 (1962).

23. Sortland, L. D. and Wilke, C. R., "Kinetics of a Dense Culture Fermentation", Lawrence Radiation Laboratory Report UCRL-18340 (1968).

24. Sortland, L. D. and Wilke, C. R., "Growth of Streptococcus faecalus in Dense Culture", Biotechnol. and Bioeng., Vol. XI, p. 805-841 (1969).

25. Theodorsen, T. and Regier, A., "Experiments on Drag of Revolving Discs, Cylinders and Streamline Rods at High Speeds", NACA Report No. 793, p. 367-384 (1945).

26. Von Karman, T., Trans. Am. Soc. Mech. Eng. 61: 705 (1939).

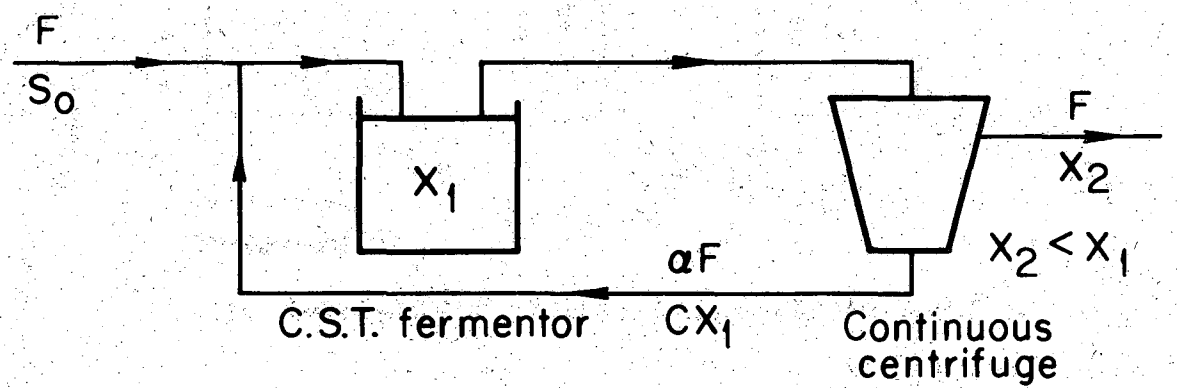

(a) C.S.T. fermentor with recycle

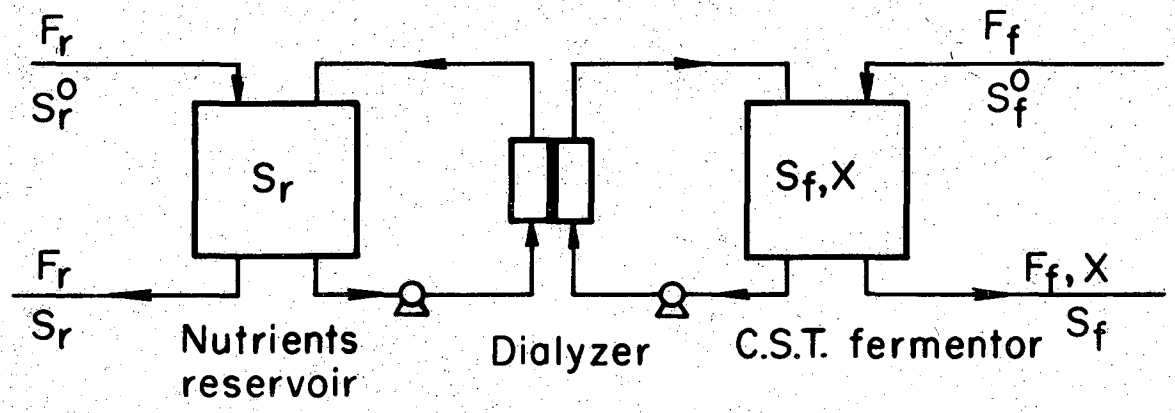

(b) Continuous dialysis fermentor system

XBL718-4044

Figure 1. High cell density culture systems.

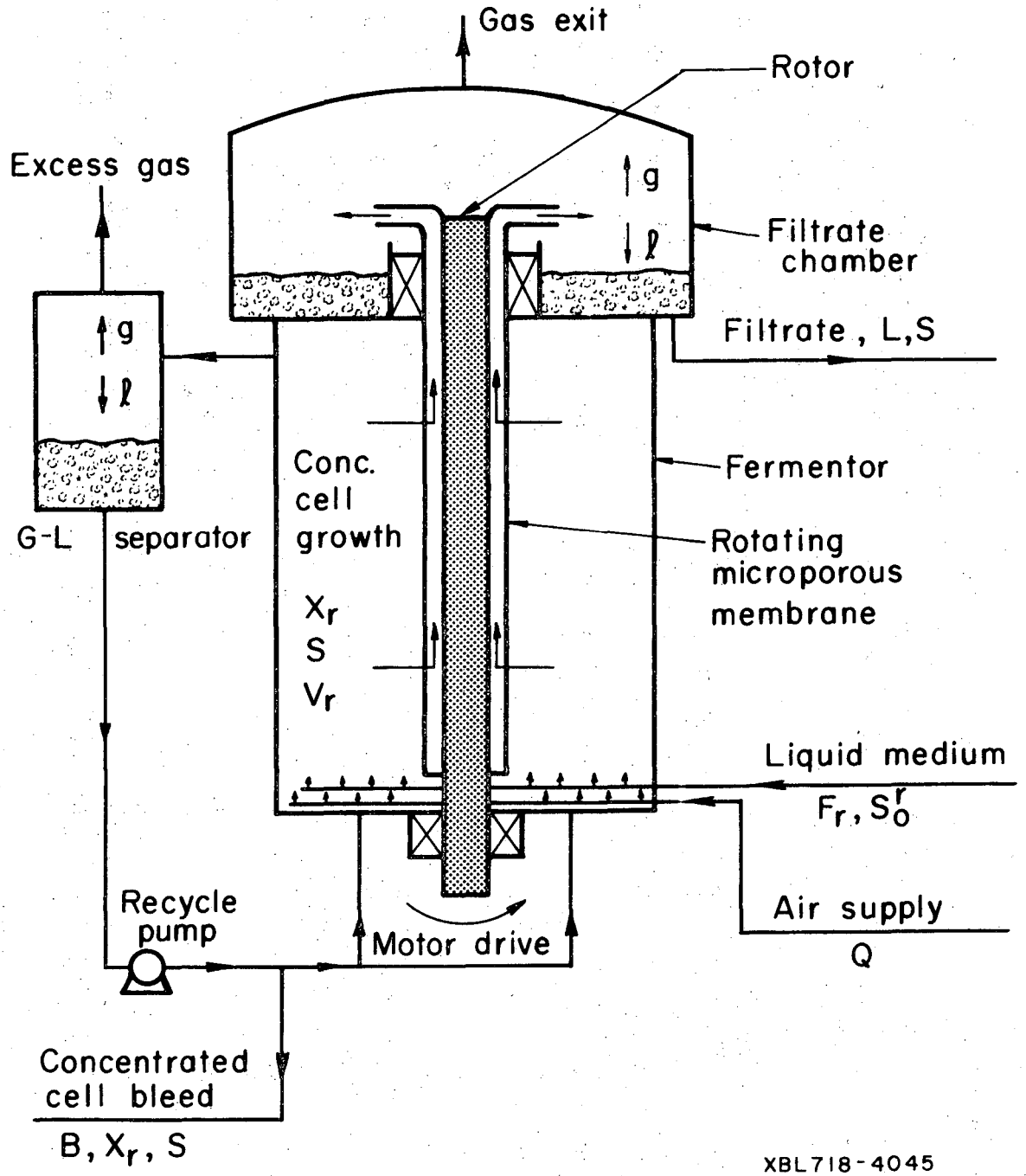

Figure 2. Schematic of the rotorfermentor assembly.

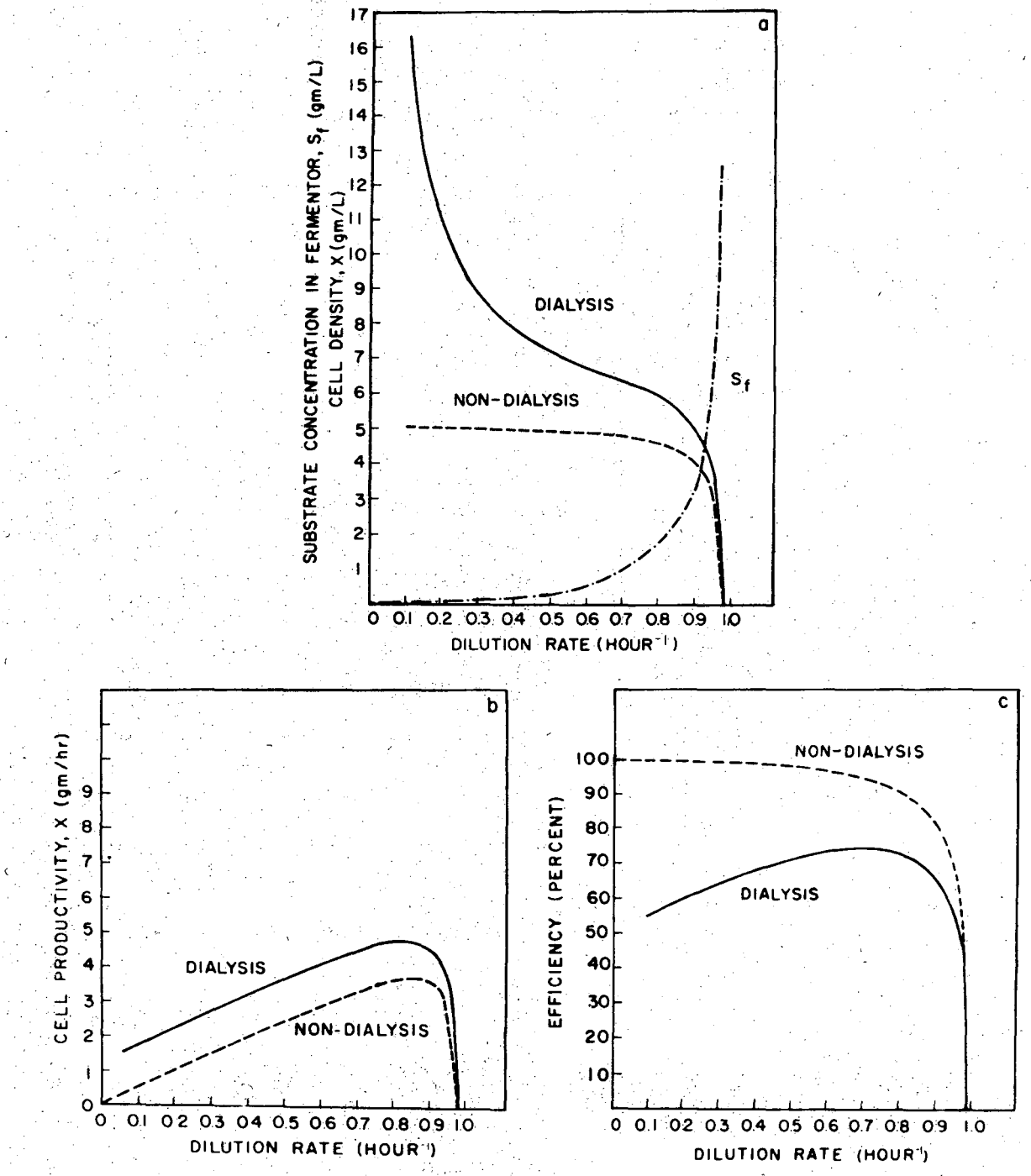

Figure 3. Calculated comparison of dialysis and nondialysis continuous culture with respect to cell density (a); productivity (b), and efficiency (c). The following conditions were assumed: fermentor volume, V_f = 1 liter; growth rate constant, μ_m = 1 hr^{-1}; growth constant, K_s = 2 × 10^{-4} g/ml; yield constant, Y_x = 0.5; maintenance constant, Y_E = 0; substrate concentration in fermentor and reservoir feed, S_r^o = S_f^o = 10^{-2} g/ml; flow rate through reservoir, F_r = 500 ml/hr; product of membrane permeability and area, $P_m A_m$ = 420 cm^3/hr. After Schultz and Gerhardt (21).

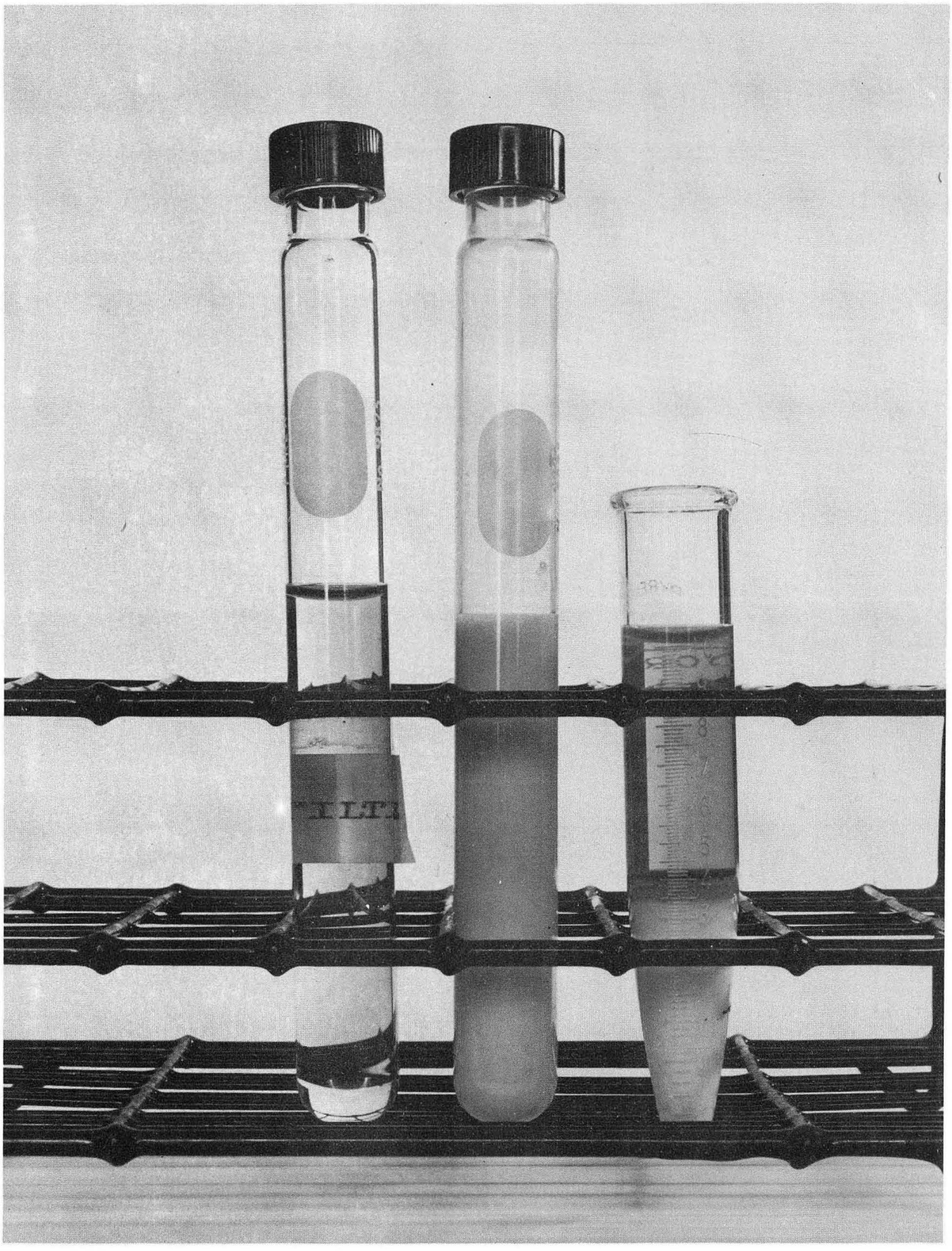

Figure 4. High density transient Run TJ. From left to right: the filtrate, the bacterial culture and a sample centrifuged at 16,000 g's for one hour which shows the 40% packed cell volume attained. After Sortland and Wilke (19). (XBB 683-1029)

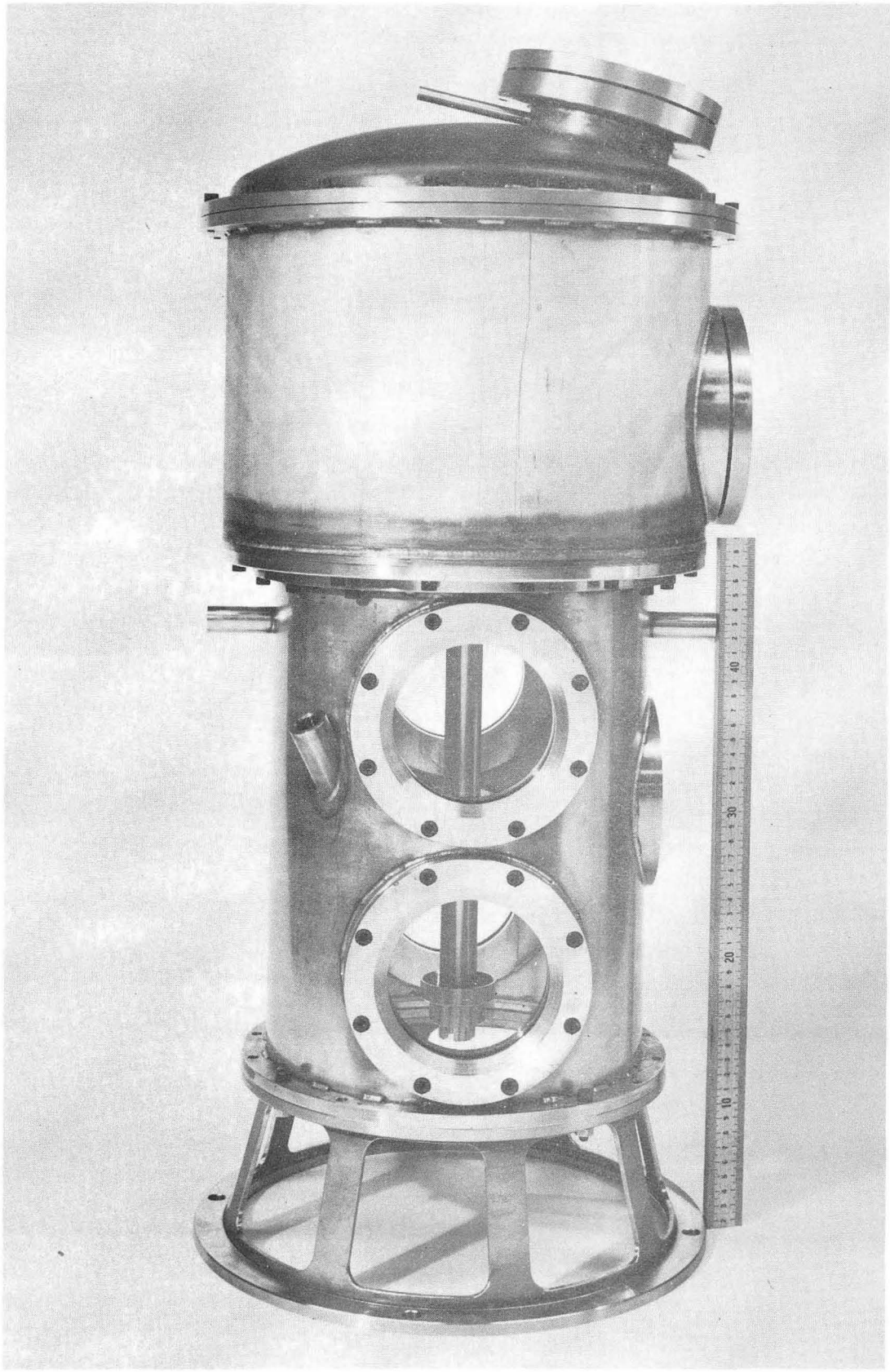

Figure 5. Rotorfermentor assembly without the filtration membrane. (XBB 718-3815)

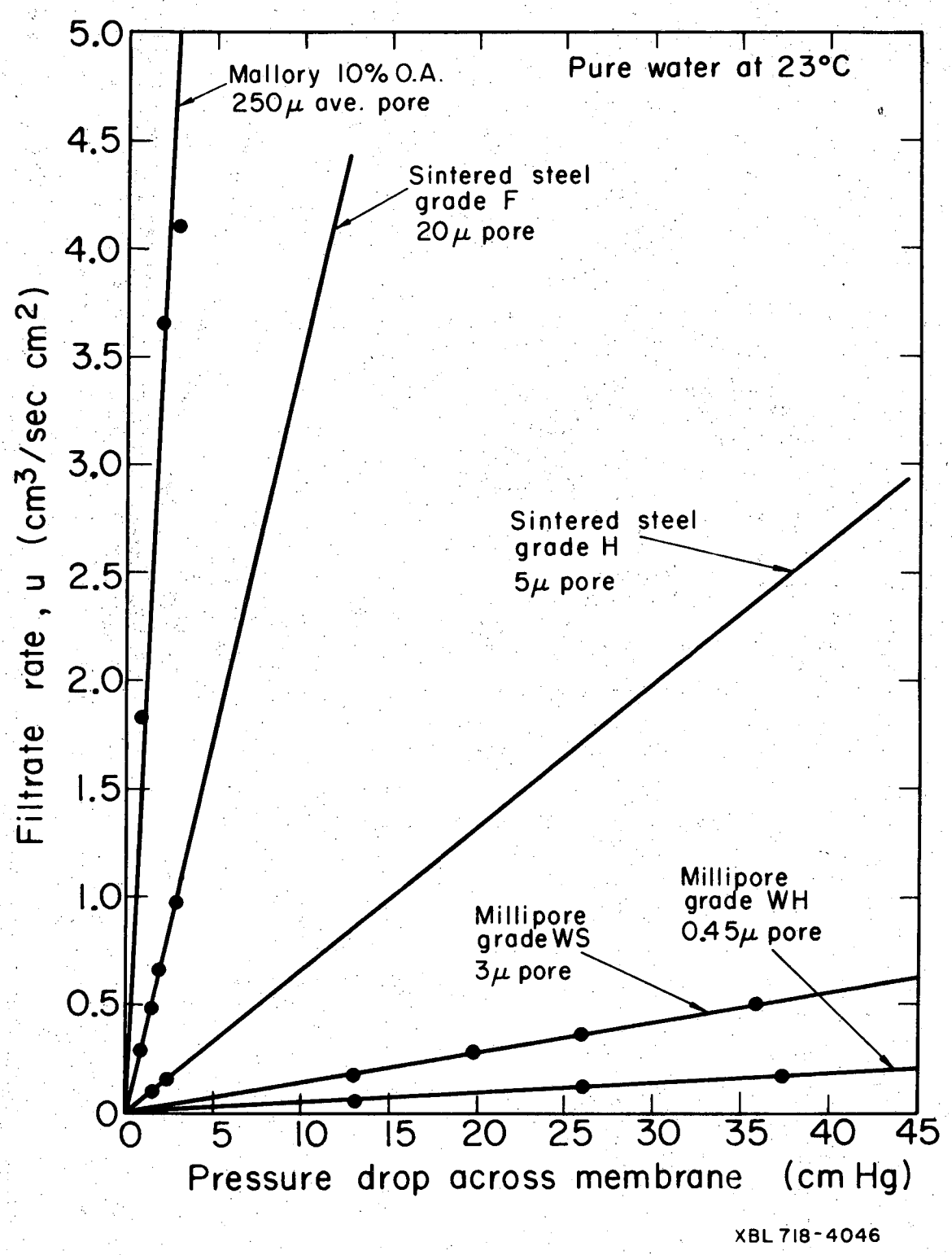

Figure 6. Filtration rates for pure water.

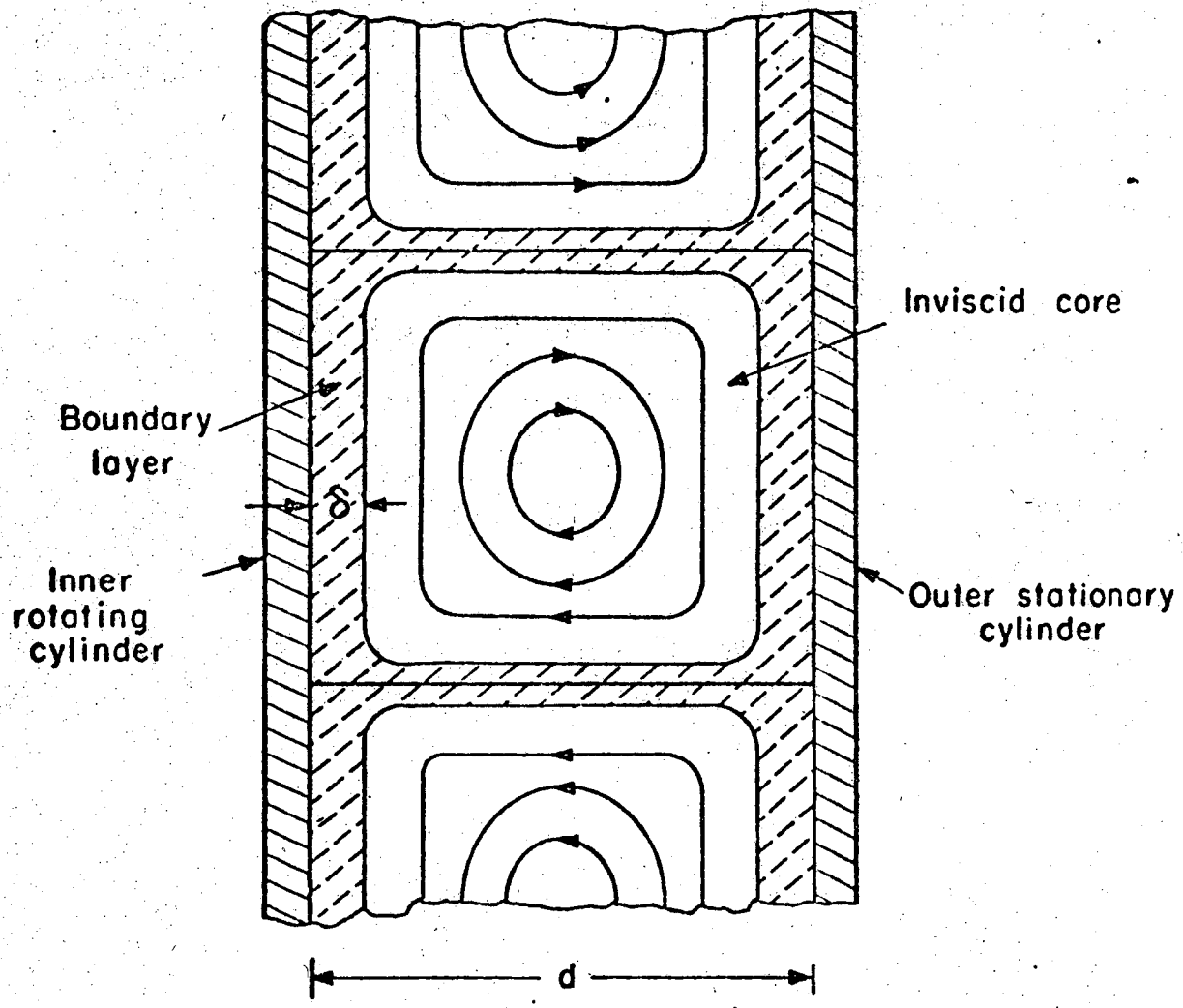

Figure 7. Flow patterns in the axial plane. After Bachelor (1).

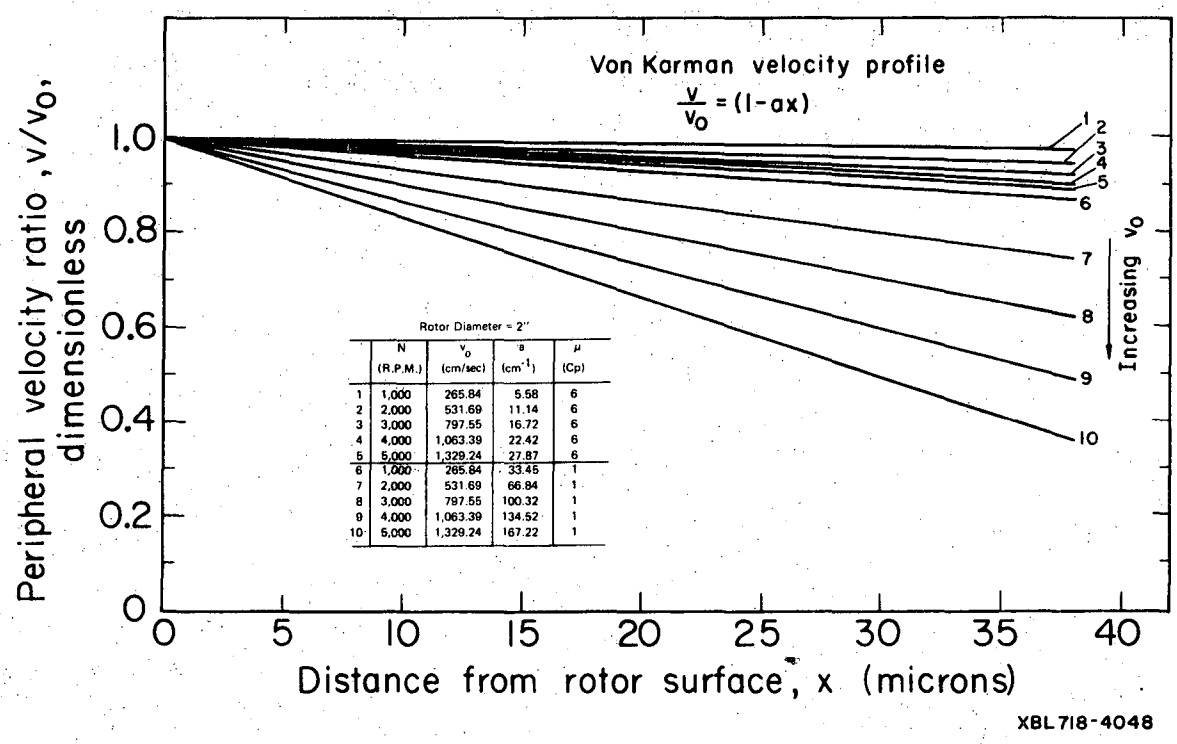

Rotor Diameter = 2"

	N (R.P.M.)	v_o (cm/sec)	a (cm^{-1})	μ (Cp)
1	1,000	265.84	5.58	6
2	2,000	531.69	11.14	6
3	3,000	797.55	16.72	6
4	4,000	1,063.39	22.42	6
5	5,000	1,329.24	27.87	6
6	1,000	265.84	33.45	1
7	2,000	531.69	66.84	1
8	3,000	797.55	100.32	1
9	4,000	1,063.39	134.52	1
10	5,000	1,329.24	167.22	1

Figure 8. Von Karman velocity profile.

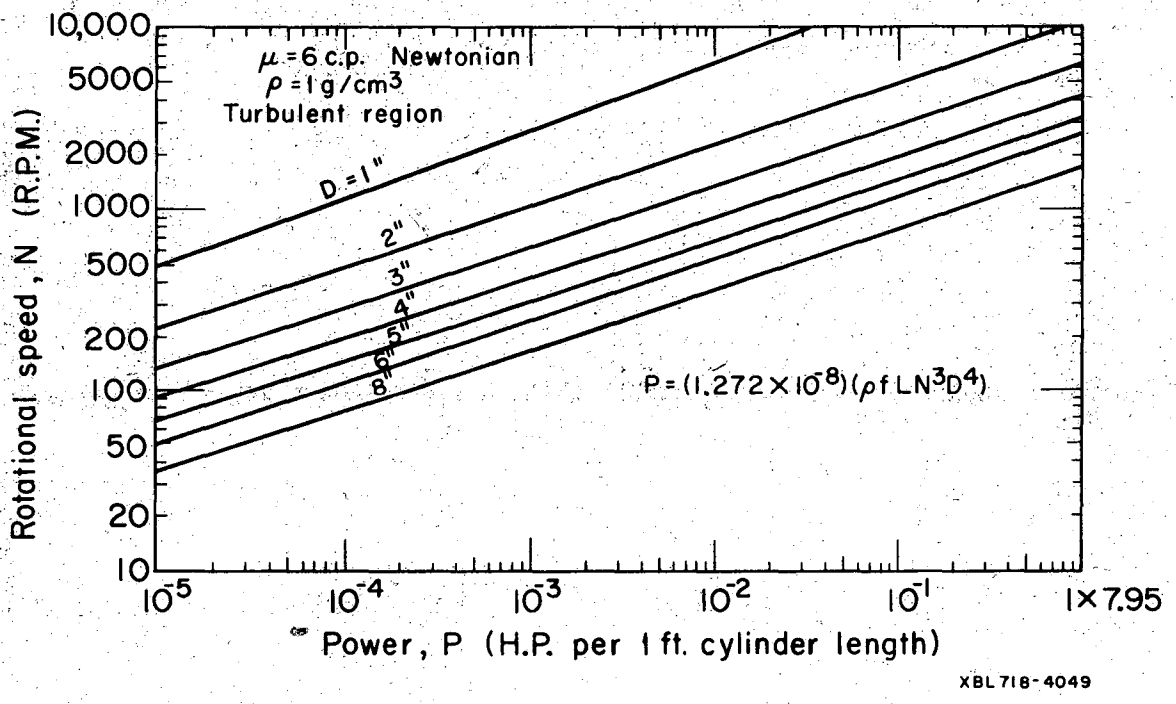

Figure 9. Power requirements of rotating cylinders (turbulent region).

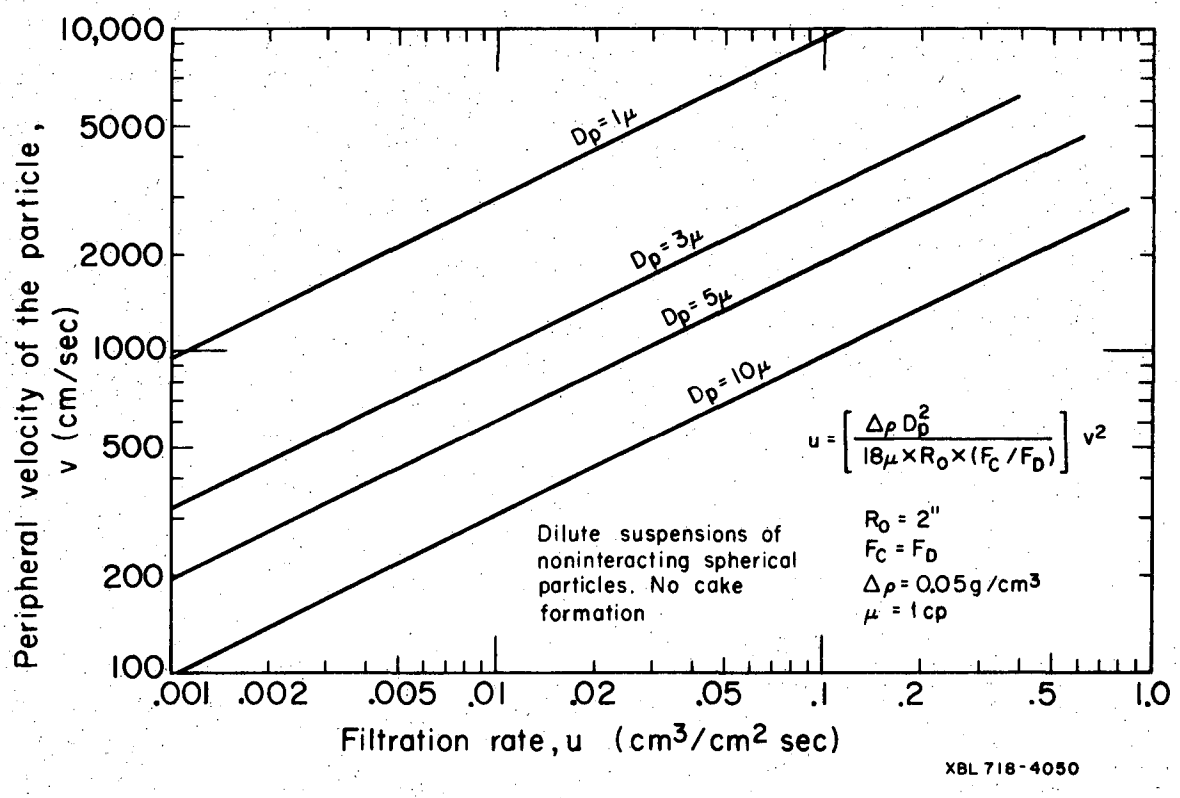

Figure 10. Filtration rates for dilute suspensions.

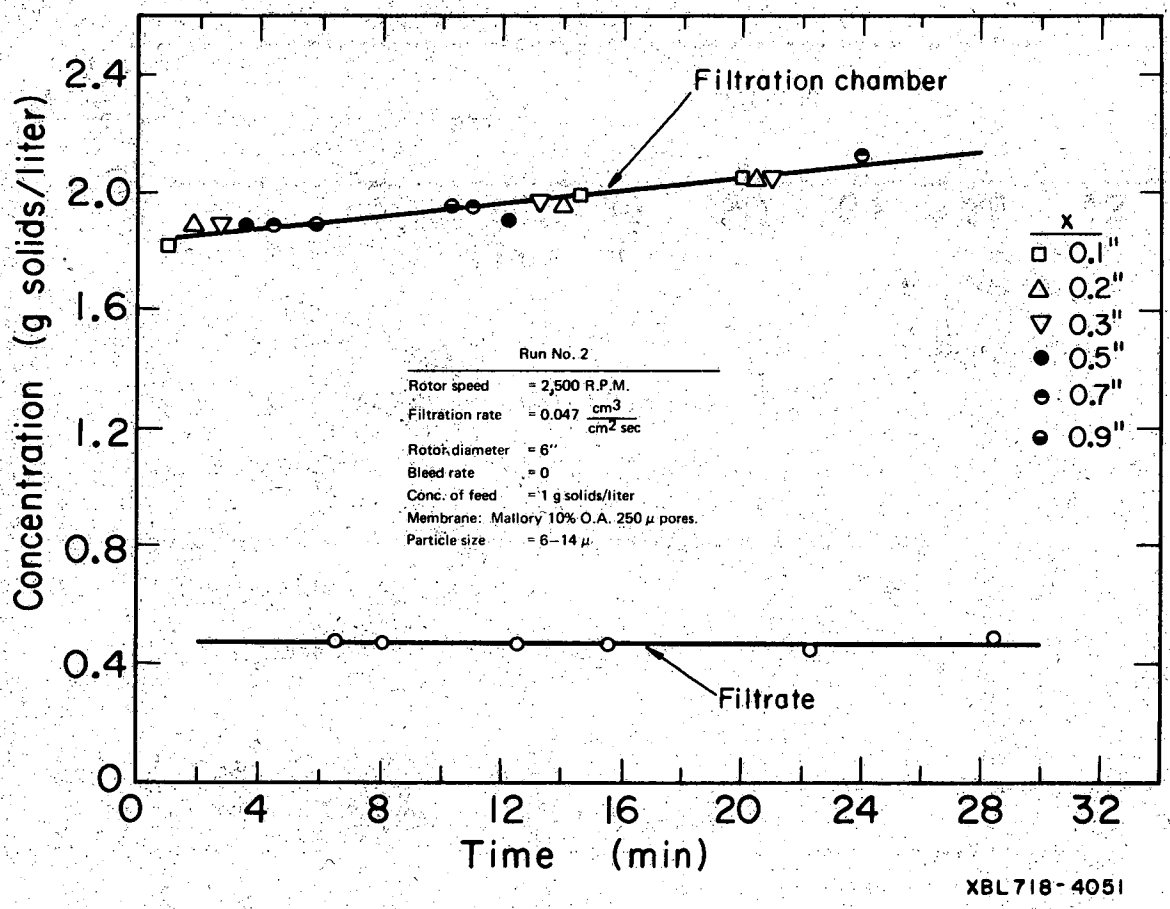

Figure 11. Filtration of dilute suspension.

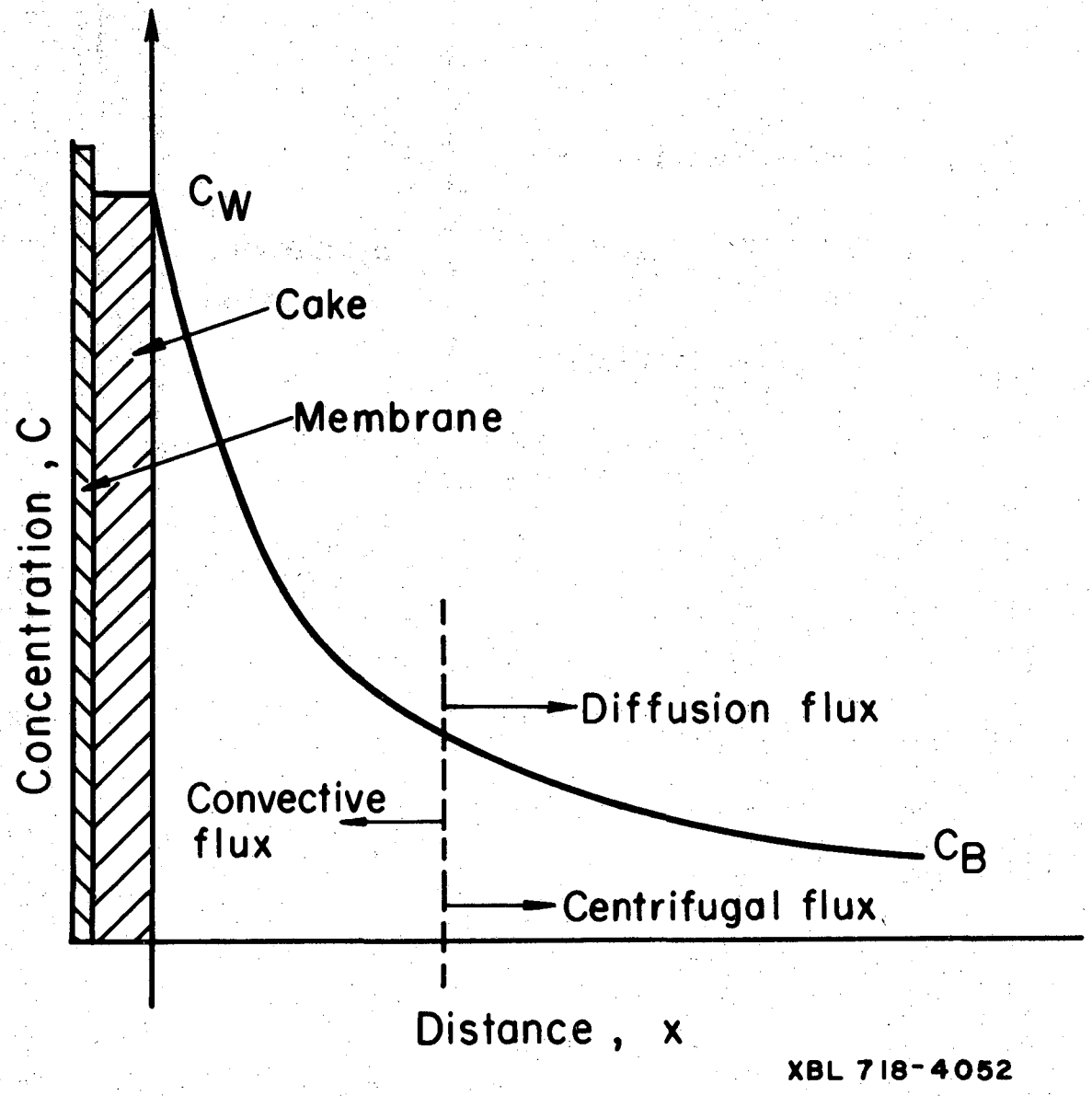

Figure 12. Theoretical model for filtration with cake formation.

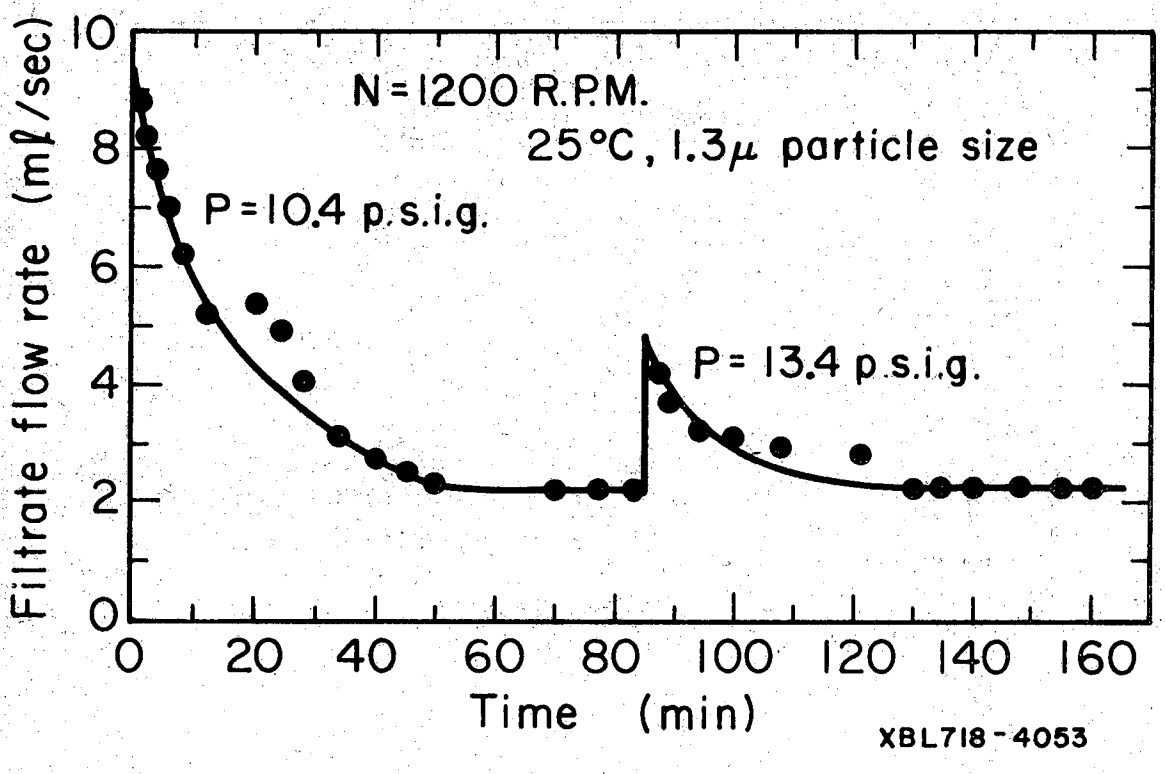

Figure 13. Filtration rate vs. time for 1.3 μ slurry at 25° C and 1200 rpm. Data of Bhagat and Wilke (2).

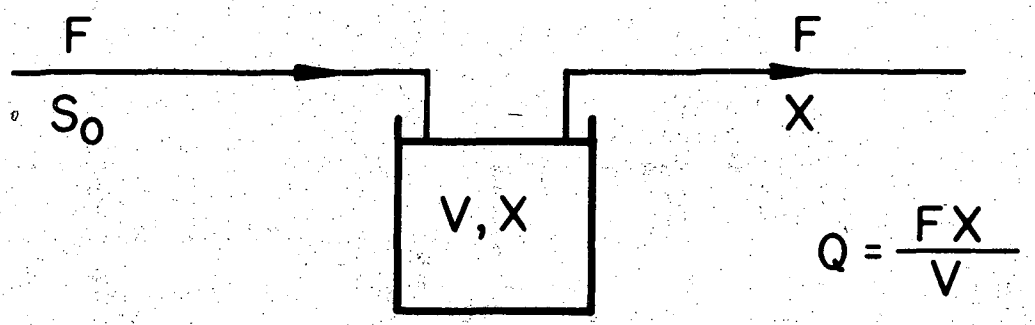

C.S.T. fermentor

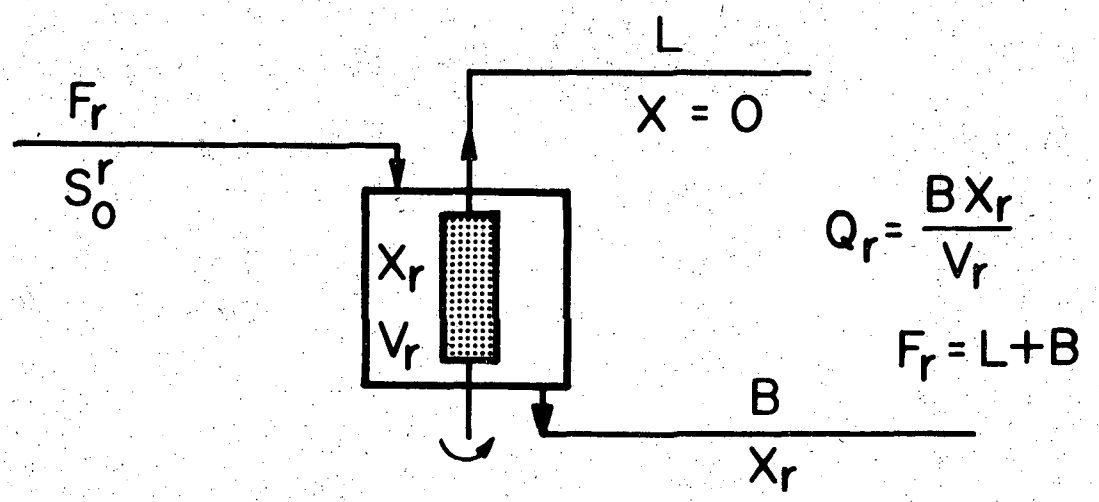

Rotorfermentor

$$R = \frac{Q_r}{Q} = \left(\frac{BV}{FV_r}\right)\left(\frac{X_r}{X}\right)$$

XBL718-4054

Figure 14. Cell productivity ratio of rotorfermentor to C.S.T. fermentor.

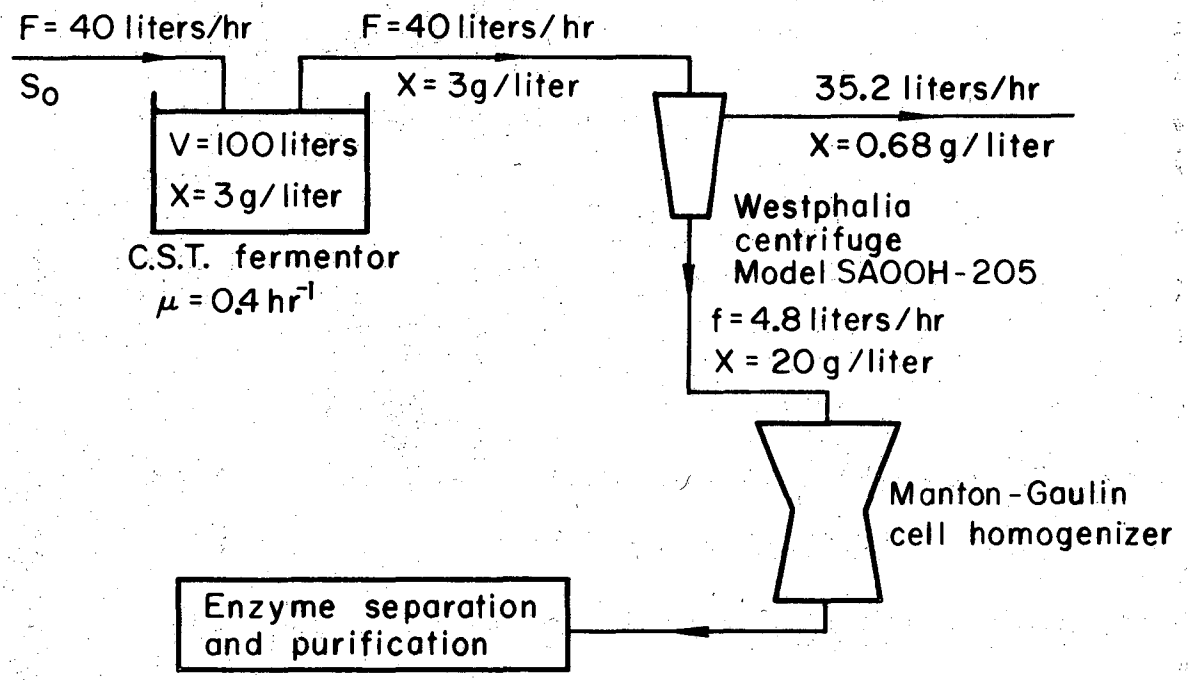

(a) Continuous amidase production

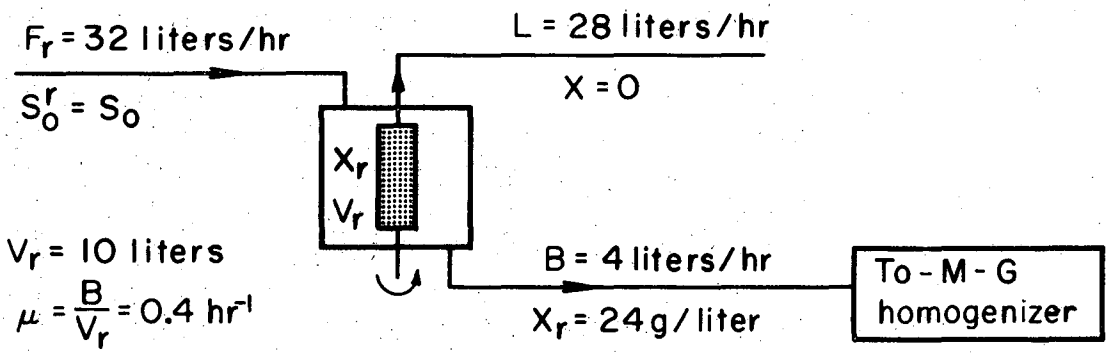

(b) Cell production and concentration by the rotorfermentor

XBL718-4055

Figure 15. Continuous endoenzyme production.

TECHNICAL INFORMATION DIVISION
LAWRENCE BERKELEY LABORATORY
UNIVERSITY OF CALIFORNIA
BERKELEY, CALIFORNIA 94720